PHYSICAL REVIEW E

STATISTICAL PHYSICS, PLASMAS, FLUIDS, AND RELATED INTERDISCIPLINARY TOPICS

THIRD SERIES, VOLUME 56, NUMBER 1 PART A JULY 1997

RAPID COMMUNICATIONS

The Rapid Communications section is intended for the accelerated publication of important new results. Since manuscripts submitted to this section are given priority treatment both in the editorial office and in production, authors should explain in their submittal letter why the work justifies this special handling. A Rapid Communication should be no longer than 4 printed pages and must be accompanied by an abstract. Page proofs are sent to authors.

Disordered waves in an excitable medium consisting of two layers: Catalytic gel and noncatalytic solution

Mario Markus, Torsten Schulte, and André Czajka
Max-Planck-Institut für molekulare Physiologie, Postfach 102664, 44026 Dortmund, Germany
(Received 28 January 1997; revised manuscript received 13 March 1997)

Disordered waves in the light-sensitive Belousov-Zhabotinsky reaction (''ripples,'' i.e., aperiodic wave front deformations, labyrinthine patterns, and ''frazzle gases,'' i.e., erratically moving wave fragments) were observed experimentally a few years ago, but have so far not been explained and modeled. The system, consisting of a gel with immobilized catalyst covered by a catalyst-free solution, is motionless and horizontally homogeneous. The observed disorder is related to enhancement or breakups of fluctuation valleys. In the model presented here, this destabilization is caused by inhibitor produced in the refractory tail that diffusively surpasses the wave front via the upper solution layer. This is in agreement with experiments both qualitatively, i.e., in the overall appearance of the patterns, as well as quantitatively, regarding the eikonal relationship and autocorrelation analysis. [S1063-651X(97)50907-X]

PACS number(s): 05.45.+b

A few years ago [1,2], we reported measurements of disordered waves in the light-sensitive Belousov-Zhabotinsky (BZ) reagent. The novelty in those reports was that disorder developed in spite of the conviction that the medium was homogeneous and motionless. These results were in contrast to reports in which hydrodynamic flow or inhomogeneities were necessary to induce disorder (see references in [1]). A more recent work [3] reports disorder resulting from convective instabilities and differing from the patterns we observed. We had reported the following transitions on increasing light intensity for sufficiently low catalyst concentrations: from smooth wave fronts to instabilities transverse to the front

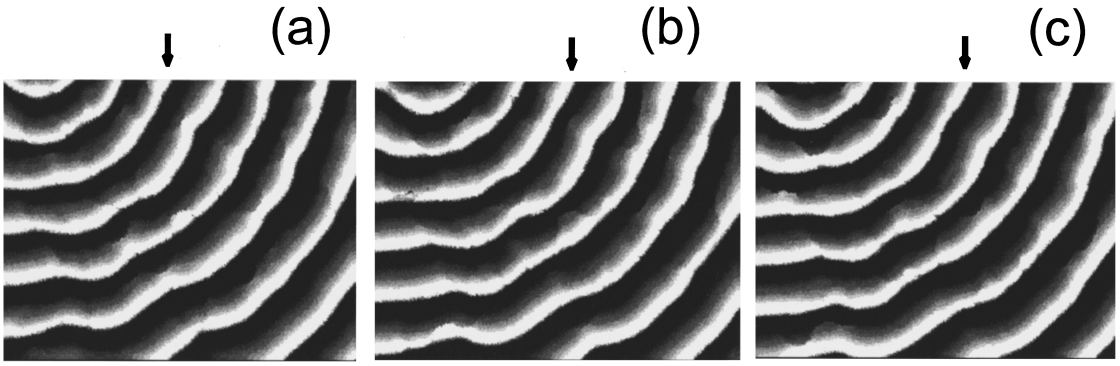

FIG. 1. Simulated ''ripples.'' The arrows indicate the same wave front at different times. Grid size: 300×225 cells. (a) 100 iterations after switching y_0 to 7. (b) 6 iterations later. (c) 18 iterations later.

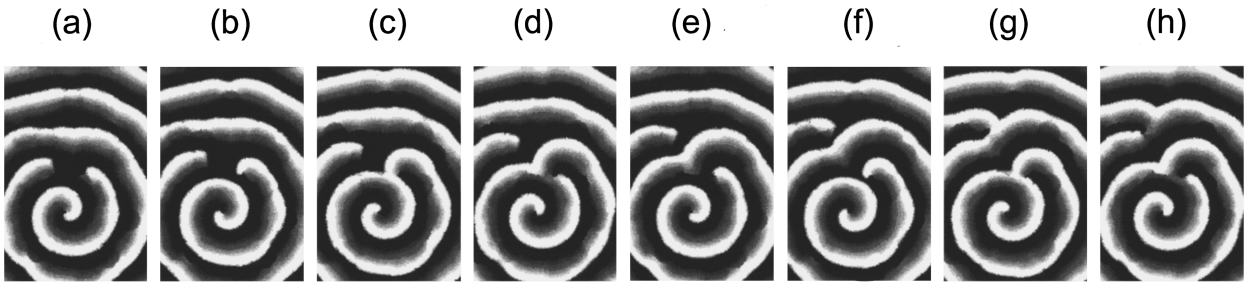

FIG. 2. Formation of a labyrinth element. Grid size: 148×225 cells. (a) 65 iterations after switching y_0 to 9. Subsequently: one picture every 5 iterations.

(''ripples''), then to breakups in the ripple valleys leading to aperiodic spirals, labyrinthine patterns, and, at very high light intensities, to erratically moving wave fragments. These fragments grew, broke, and annihilated by collisions with each other, sustaining a global disordered state (''frazzle gas''). Disordered modes with unchanged global properties could be observed during times lasting up to 1.5 h.

So far, to our knowledge, no adequate mechanism has been proposed for these aperiodicities. The destabilizing mechanism discussed by Horváth *et al.* [4] is to be discarded as it involves the consumption of a reactant in front of the wave, but the relevant reactants are in our case so highly concentrated that they are not rate determining. In Ref. [2], we also considered the mechanism proposed by Kuramoto [5]. He assumed that the inhibitor (produced in the refractory tail of the wave) diffuses faster than the activator (produced in the front); thus, distortions of the wave back are smoother than distortions of the front, resulting in the appearance of inhibitor in the front of activator valleys, which leads to valley retardation, i.e., to structure enhancement. This mechanism requires that the inhibitor (here Br^-) moves through the activator front (here $HBrO_2$) until it surpasses the front at the valleys (see Fig. 12 in Ref. [2]). However, by virtue of the very fast and almost irreversible $HBrO_2$-Br^- annihilation (reaction $R2$ in Ref. [6]), $HBrO_2$ and Br^- cannot coexist for typical times of the wave dynamics, so that the idea of Br^- tunneling through $HBrO_2$ is unrealistic.

Our experimental setup [1] consisted of a silica gel in a Petri dish, in which the catalyst (ruthenium bipyridyl complex) was immobilized. Above the gel, there was a solution layer (having equal dimensions as the gel) containing all BZ reactants except the catalyst. We recently noticed that this solution layer is essential for the occurrence of disordered patterns. We thus must take into consideration inhomogeneities in the vertical direction, while we retain the conviction that there is horizontal homogeneity and zero dynamic flow. Recently, we corroborated the absence of flow as follows. We mixed black pigment particles (supplied by F. Schoenfeld, Düsseeldorf; mean diameter: 0.5 μm) in the solution layer above the gel and measured their positions at different depths with a microscope by adjusting its focus. For the setup in [1] no particle motion was observed; for control, we doubled the depth of the layer, and did detect convective motion. A further indication that there is no flow is the observation of unperturbed spirals at low light intesities [1,2].

Considering the vertical direction, we now apply Kuramoto's ideas in a modified form: Br^- surpasses $HBrO_2$ via an upper-layer detour. This is possible at sufficiently high light intensities, since it is known that light produces Br^- [7]. $HBrO_2$, which is maintained at a high value by autocatalysis at the wave front in the gel, reaches the upper layer by diffusion and is there substantially decimated by photochemically produced Br^-. This allows the excess Br^- produced in the refractory wave tail to surpass the wave front diffusing through an $HBrO_2$-free region in the upper solution. Retardation of fluctuation valleys occurs by Br^- concentration enhancement due to the concave geometry, which implies converging vectors of diffusive flow of Br^-. Contrarily, fluctuation crests are less retarded, as the convex geometry causes divergence of flow vectors.

We formalize these ideas by constructing a cellular au-

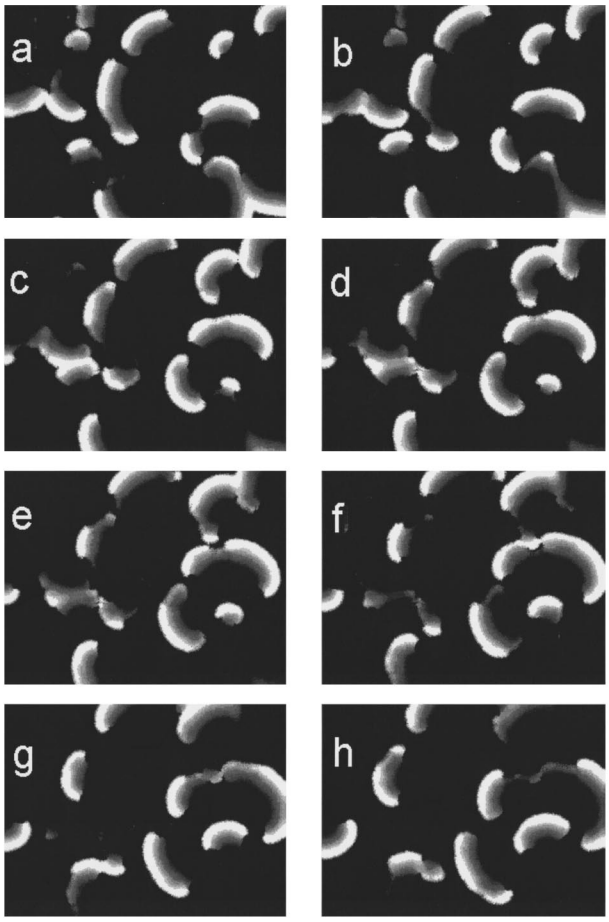

FIG. 3. Simulated ''frazzle gas.'' Grid size: 300×225 cells. (a) 300 iterations after switching y_0 to 10. Subsequently: one picture every 4 iterations.

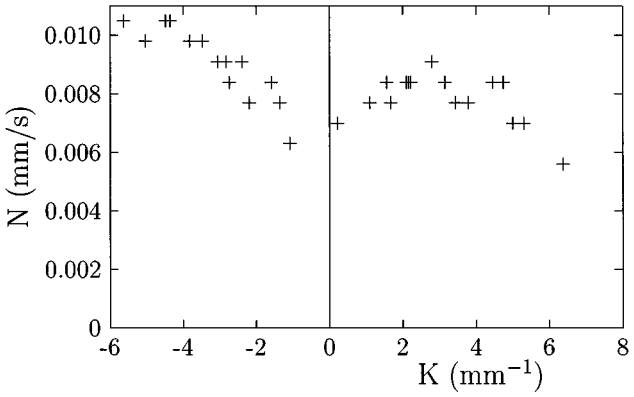

FIG. 4. Normal wave-front velocity N vs wave-front curvature K, as obtained from simulated ripples [$(y_0=7;\ K>0$ ($K<0$), means convex (concave) waves].

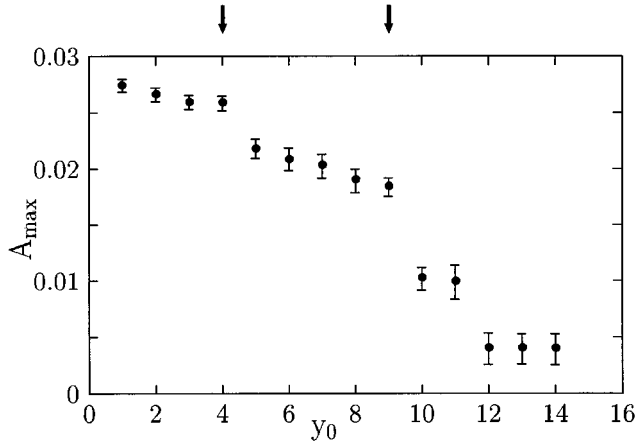

FIG. 5. Simulated maximum of the autocorrelation function $A_{\max}$ vs steady state inhibitor concentration y_0 (dimensionless quantities). The left (right) arrow indicates the transition from a smooth spiral to ripples (from ripples to a frazzle gas). Circles indicate the average over 150 iterations. Error bars: amplitude of temporal oscillations of $A_{\max}$.

tomaton with a quasistochastic geometry, which guarantees isotropic wave propagation and has rendered quantitative agreement with experiments [8]. While in [8] two variables were enough, we must consider here a third variable, namely, Br^-. The variables now are as follows: x, $HBrO_2$ concentration; y, Br^- concentration; and z, concentration of the oxidized catalyst. Intermediate values between iterations are defined as follows: $x\rightarrow x'\rightarrow x''\rightarrow x$, $y\rightarrow y'\rightarrow y''\rightarrow y'''\rightarrow y$, $z\rightarrow z'\rightarrow z$. In the gel, we use the following rules: (i) If $x>0$ and $z<z_{\max}$, then $x'=\alpha x$, $y'=0$, $z'=z+\gamma x$; (ii) if $x>0$ and $z=z_{\max}$, then $x'=0$, $y'=\kappa z$, $z'=z-\beta z$; (iii) if $x=0$, then $x'=0$, $y'=\kappa z$, $z'=z-\beta z$. Both in the gel and in the upper solution, we use the following rules: (iv) If $(\langle x'\rangle-\langle y'\rangle)>0$, then $x''=\langle x'\rangle-\langle y'\rangle$, $y''=0$, else $y''=\langle y'\rangle-\langle x'\rangle$, $x''=0$; (v) if $y'>0$, then $y'''=y''+\rho(y_0-y'')$. The angular brackets denote averaging over a neighborhood of radius R. The variables are rounded to the next integer after each step. The parameters are α, $z_{\max}$, γ, β, κ, R, ρ, and y_0.

Rule (i) describes the active front, in which x is produced autocatalytically, annihilating y and oxidizing the catalyst (reactions $R5$, $R6$, and $R2$ in [6]). Rule (ii) describes the transition from the wave front to the refractory tail, as full oxidation of the limited amount of catalyst ($z=z_{\max}$) causes a sharp cutoff of x at the back of the active front. Here, and in the refractory tail [described by rule (iii)] the reduced catalyst ($z-z_{\max}$) is regenerated, while y (produced by the remaining z) annihilates x (reactions $R9$, $R10$ in [6]). Note that we have simplified the x (or y) profile by a step function jumping from zero (or jumping down to zero) at the point where $z=z_{\max}$. In steps (iv) and (v) we consider the diffusion of x and y by averaging over the circular neighborhood of radius R, as well as activator-inhibitor annihilation. We assumed that for a given light intensity, a steady-state inhibitor concentration y_0 is asymptotically established; any changes (y_0-y'') due to the wave dynamics relax towards y_0 by virtue of rule (v).

Agreement between calculations and experiments was obtained after parameter optimization, yielding the following values, which were used throughout this work: $\alpha=2$, $z_{\max}=10$, $\gamma=0.2$, $\beta=0.3$, $\kappa=4$, $R=4$, and $\rho=0.2$. As a control paramter, we varied y_0, which is correlated to the light intensity. As an initial condition, we always started with a spiral that had developed over the whole grid for 200 iterations and $y_0=4$; this corresponds to the experimental initial condition, in which a spiral was initially allowed to develop over the whole Petri dish in the dark. The simulations showed that in an upper layer whose thickness is reduced below one-half, there is enough $HBrO_2$ to prevent Br^- from surpassing the wave front; consequently, no disorder develops. This corroborates quite well with experiments: disorder turns into smooth waves when thinning of the upper layer crosses a threshold of 45%.

The results are shown in Figs. 1–5. In Figs. 1–3, white corresponds to $z=z_{\max}$ and black to $z=0$. Figure 1 shows ''ripples'' at relatively low light intensities ($y_0=7$). The fluctuations that are enhanced via transverse instabilities are given by the quasistochasticity of the automaton point distribution. Figure 2 shows the formation of a labyrinth element for a higher light intensity ($y_0=9$) and sufficiently small wavelengths. Here, ripple valleys can have such a high curvature that inhibitor flow vectors converge strongly enough to break the waves. Spatial aperiodicities cause here the excitability to be higher at the right than at the left open wave end [Fig. 2(a)]; thus, the right end curls earlier to a spiral than the left one. The refractory tail of the right spiral breaks the preceding wave front [Figs. 2(d) and 2(e)], while the retarded left one does the same with a different front later on [Fig. 2(h)]. Future calculations with larger grids should readily yield more extended and complex labyrinths, as in experiments [1,2]. For even higher light intensities (Fig. 3; $y_0=10$) wave fronts break more often than in Fig. 2 and, just as in experiments, wave pieces change their length without spiraling, while collisions annihilate them. The resulting aperiodic ''frazzle gas'' does not change qualitatively, i.e., in its overall appearance, in time.

Quantification of our results, for comparison with experiments, are given in Figs. 4 and 5. Figure 4 shows the eikonal relationship, as determined from the simulation of ripple formation. For stable waves in excitable media, the normal velocity N monotonically decreases with the curvature K [9–11], implying that fluctuations in K are smoothed out.

Here, however, a branch with $dN/dK>0$ destabilizes the fronts, while the branches with $dN/dK<0$ restrict the ripple amplitude. In order to increase significance, analyses were performed at varying positions of the grid, causing the scatter of the points in Fig. 4. The agreement of this figure with the experimental diagram in [2] is excellent. This agreement was made quantitative by fixing the axis numbering in Fig. 4 through the following calibration: 1 automaton iteration=2 s, 1 cell edge length=42 μm. For a test of the model, we applied this calibration to a simple spiral for $y_0=4$: the spiral period T (21 iterations) yields 42 s, while its wavelength λ (40 cells) yields 1.68 mm. This agrees well with experimental values for spirals in the dark: $T=40-50$ s, $\lambda=1.5-1.8$ mm.

As a further quantification, we determined the spatial correlation function A of the variable z, using the same algorithm as in Ref. [1]. The maximum $A_{\max}$ is given in Fig. 5 as a function of y_0, agreeing fairly well with the corresponding diagram in [1]. Comparison of the simulated with the experimental diagrams allows an approximate calibration: $y_0=1$ corresponds to a light intensity of $I\approx 40$ mW/m^2. Note that the locking of $A_{\max}$ to a fixed value at each type of mode, as obtained in experiments, is less pronounced in simulations.

Recent results [12] have shown that an excess of oxygen (above that of air) at relatively low light intensities produces the same patterns as those given in [1,2] for higher light intensities in air. This is explained by oxygen-induced Br^- production [13,14]. As far as we can presently judge, the model in this work is applicable to this phenomenon if we consider y_0 to be dependent on both light intensity and oxygen concentration.

We acknowledge the financial support of the Deutsche Forschungsgemeinschaft (Grant Nos. MA 629/4-1 and MA 629/4-2).

[1] M. Markus, G. Kloss, and I. Kusch, Nature (London) **371**, 402 (1994).
[2] M. Markus and K. Stavridis, Int. J. Bifurcation Chaos Appl. Sci. Eng. **4**, 1233 (1994).
[3] Q. Ouyang and J.-M. Fleselles, Nature (London) **379**, 143 (1996).
[4] D. Horváth, V. Petrov, S. K. Scott, and K. Showalter, J. Chem. Phys. **98**, 6332 (1993).
[5] Y. Kuramoto, Prog. Theor. Phys. **63**, 1885 (1980); *Chemical Oscillations, Waves and Turbulence* (Springer, Berlin, 1984), Chap. 7.
[6] J. J. Tyson, in *Oscillations and Travelling Waves in Chemical Systems*, edited by R. J. Field and M. Burger (Wiley, New York, 1985), Chap. 3.
[7] L. Kuhnert, Nature (London) **319**, 393 (1986).
[8] M. Markus and B. Hess, Nature (London) **347**, 56 (1990).
[9] J. P. Keener and J. J. Tyson, Physica D **21**, 307 (1986).
[10] P. F. Foerster, S. C. Müller, and B. Hess, Proc. Natl. Acad. Sci. USA **86**, 6831 (1989).
[11] V. S. Zykov and O. L. Morozova, Biophysics **24**, 739 (1980); V. S. Zykov, *ibid.* **25**, 906 (1980).
[12] A. Czajka and M. Markus (unpublished).
[13] H. Sutin and C. Creutz, Pure Appl. Chem. **52**, 2717 (1980).
[14] M. K. Ram Reddy, Z. Szlavik, Zs. Nagy-Ungvarai, and S. C. Müller, J. Phys. Chem. **99**, 15 081 (1995).